International Journal of Mechanical, Industrial and Aerospace Sciences
ISSN: 2517-9950
Vol:8, No:8, 2014

Material Characterization and Numerical Simulation of a Rubber Bumper

Tamás Mankovits, Dávid Huri, Imre Kállai, Imre Kocsis, Tamás Szabó

***Abstract*—**Non-linear FEM calculations are indispensable when important technical information like operating performance of a rubber component is desired. Rubber bumpers built into air-spring structures may undergo large deformations under load, which in itself shows non-linear behavior. The changing contact range between the parts and the incompressibility of the rubber increases this non-linear behavior further. The material characterization of an elastomeric component is also a demanding engineering task. In this paper a comprehensive investigation is introduced including laboratory measurements, mesh density analysis and complex finite element simulations to obtain the load-displacement curve of the chosen rubber bumper. Contact and friction effects are also taken into consideration. The aim of this research is to elaborate a FEM model which is accurate and competitive for a future shape optimization task.

***Keywords*—**Rubber bumper, finite element analysis, compression test, Mooney-Rivlin material model.

I. Introduction

THE rubber bumpers built into air-spring structures of buses perform a number of critical tasks. They are working together with the air-spring as a secondary spring, thus modifying the original characteristics of the air-spring when pressed together. When the bus is in a stationary position and settles to the ground, the static weight of the chassis and the body rests on the bumper. If the fibre-reinforced bellow of the air-spring wears through while the bus is running, the vehicle can safely reach the nearest garage at a limited speed while bouncing on the bumper, and no additional damage will occur. It prevents metal-on-metal collision at large dynamic impulses and absorbs the impulse. These rubber bumpers are subjected to compressive stress, for which the characteristics shows a progressive feature [1]. Consequently, their finite element analysis requires considerable effort.

The literature does not devote much room to the examination of the rubber bumpers of air-springs. A finite element code was introduced for the numerical analysis of axi-symmetric rubber bumpers [2], [3]. Another area where rubber mounts are used is the flexible support of engines, on which several works have been published. Estimation of the fatigue life of rubber springs, rubber mounts and air springs is carried out in [4]-[7]. In [8] extensive studies on the rubber mounts of engines are performed using the finite element method.

This research intends to determine the behavior of the rubber bumper in the complete range of operation. The paper also deals with the indispensable uniaxial compression test under laboratory conditions considering the ISO 7743 standard. The laboratory measurements are used to determine the numerical material parameters for the finite element analysis. Numerical analysis is performed to obtain the optimal input parameters for the proper and fast calculations such as mesh density and bulk modulus. The measurement results and the finite element calculations are also compared to validate the FEM model.

II. Material Characterization

The successful finite element simulation of rubber parts hinges on the selection of an appropriate strain energy function and on the accurate determination of material constants. The ISO 7743 standard [9] specifies methods for the determination of the compression stress-strain properties of vulcanized rubber using a standard test piece or a product. According to the standard four test pieces (cylinder of diameter 29 ± 0.5 mm and height 12.5 ± 0.5mm) were cut from the rubber part examined, see in Fig. 1.

Fig. 1 The rubber bumper, the test pieces and the compression test

The compression tests with a film of lubricant were done and the stress-strain properties were evaluated. The characteristics of a test piece can be seen in Fig. 2.

Tamás Mankovits and Dávid Huri are with the Department of Mechanical Engineering, University of Debrecen, H-4028 Hungary (phone: +36-52-415-155, e-mail: tamas.mankovits@eng.unideb.hu, huri.david@eng.unideb.hu).

Imre Kállai is with the Institute of Polymer Product Engineering, Johannes Keppler University Linz, A-4040 Austria (phone: +43-732-2468-6654, e-mail: imre.kallai@jku.at).

Imre Kocsis is with the Department of Basic Technical Studies, University of Debrecen, H-4028 Hungary (phone: +36-52-415-155, e-mail: kocsisi@eng.unideb.hu).

Tamás Szabó is with the Institute of Machine Tools and Mechatronics, University of Miskolc, H-3515 Hungary (phone: +36-46-565-111, e-mail: szabo.tamas@uni-miskolc.hu).

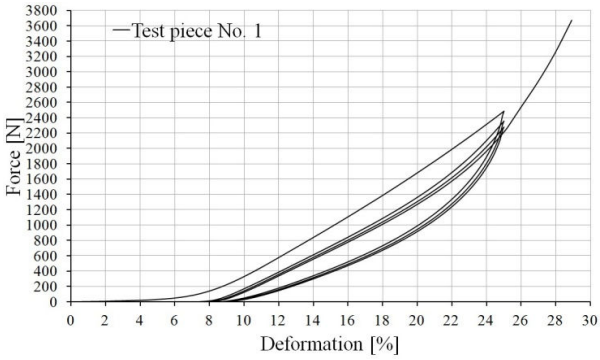

Fig. 2 The force-deformation curves of the test piece

The force-deformation curve shows clearly the pre-loading cycles applied during the measurement and the essential segment (belonging to the fourth loading) providing information about the elastic properties of the rubber part. It can be seen that the hysteresis losses are decreasing during the consecutive cycles and tending to a limit and finally the system reaches its steady-state deformation. Since additional compression occurs due to the geometrical errors at the beginning of measurements, the values of the deformation have to be corrected for the further calculations. The actual compression modulus of the rubber can be determined from the force-deformation curve obtained as a result of the fourth loading [9]. These actual compression modulus values are necessary for the calculation of the actual stresses at different strains. In the evaluation the investigated rubber was supposed to be incompressible. Considering frictionless contact between the rubber part and the steel plates the stress-strain curve that is needed for the calculation of the numerical material constants can be determined, see in Fig. 3.

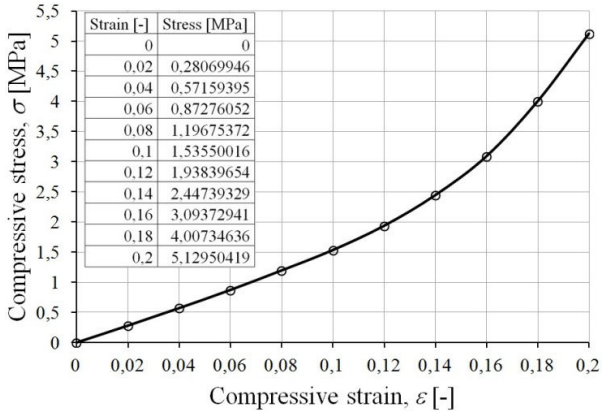

Fig. 3 The rubber characteristics

For rubber the material models are given by the strain energy function. This function of nearly incompressible materials can be divided into a volume-changing and a volume-preserving part. The strain energy density resulting from the change in volume $U(J)$ is given in the following form:

$$U(J) = \frac{1}{2} \cdot \kappa \cdot (J-1)^2, \quad (1)$$

where J is the Jacobian, κ is the bulk modulus, which is a real material characteristic. If an incompressible material is examined then $U(J)$ is zero, which mean $\nu = 0.5$. It is to be noted that rubber bumpers may be regarded as nearly incompressible materials due to additives. Accordingly, the Poisson ratio is between $0.49 < \nu < 0.5$.

A number of material models can be found in the literature for the volume-preserving member of strain energy density. In our investigations the 9 term Mooney-Rivlin material model is used to describe the material behavior, where the strain energy density is expressed using the scalar invariants:

$$W(\boldsymbol{C}) = C_1(I_I - 3) + C_2(I_{II} - 3) + C_3(I_I - 3)^2 + C_4(I_I - 3)(I_{II} - 3) + C_5(I_{II} - 3)^2 + C_6(I_I - 3)^3 + C_7(I_I - 3)^2(I_{II} - 3) + C_8(I_I - 3)(I_{II} - 3)^2 + C_9(I_{II} - 3)^3 \quad (2)$$

where I_I and I_{II} are the first and the second scalar invariants of the volume preserving member of the Cauchy-Green strain tensor of the right $\boldsymbol{C}$, $C_1, C_2, C_3, C_4, C_5, C_6, C_7, C_8$ and C_9 are the Mooney-Rivlin material constants.

A non-linear curve fitting procedure using software ADINA was done to determine the Mooney-Rivlin material constants (see in Fig. 4) and FEMAP was used for the control finite element calculation.

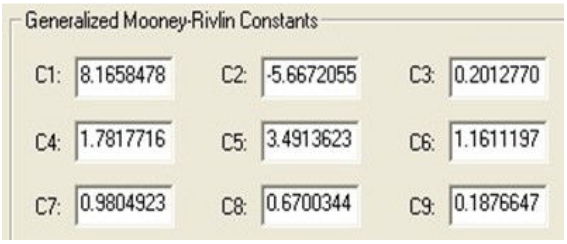

Fig. 4 Mooney-Rivlin material parameters determined by the ADINA

Using the material parameters determined by the ADINA the FEMAP results showed very good agreement with the laboratory measurement, see in Fig. 5.

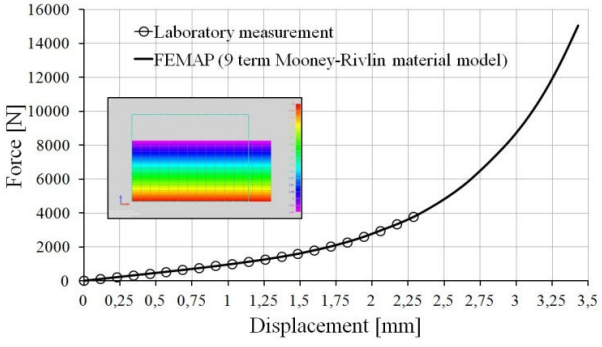

Fig. 5 Control calculation carried out using FEMAP

III. Finite Element Analysis of the Rubber Bumper

According to the ISO 7743 standard the rubber bumper was also compressed using INSTRON biaxil testing machine. The original geometry of the rubber bumper and its compression test in frictionless conditions are shown in Fig. 6.

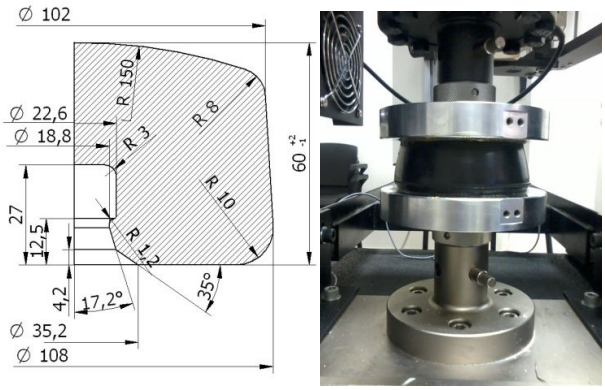

Fig. 6 Geometry of the rubber bumper and its compression test

The load-displacement curve for pressure is known from the measurement but only when the bumper is loaded between two flat rigid surfaces. We had to take into consideration that fast but accurate finite element calculations were needed to realize an effective optimization task. A numerical analysis was needed to obtain the optimal input parameters for the finite element analysis such as mesh density and bulk modulus [2]. The initial gap between the upper plate and the rubber was 1mm. The deformation of the rubber bumper at 24mm compression can be seen in Fig. 7.

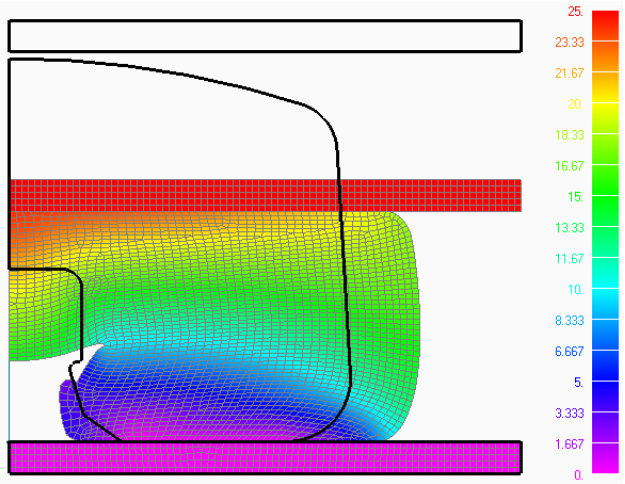

Fig. 7 The initial and the deformed geometry

The measurement and the simulation were compared, see in Fig. 8.

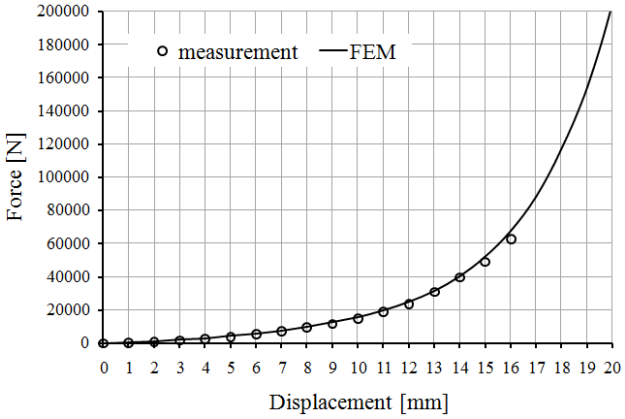

Fig. 8 The load-displacement curve

To determine the clearest mesh the accuracy of the solution has been analyzed. The effect of the mesh density change was compared at two discrete points (12mm and 24mm compression). The error

$$\varepsilon(\%) = \frac{\sqrt{(F_{ref}-F)^2}}{F_{ref}} \cdot 100 \qquad (3)$$

where F_{ref} is the compressive force for the reference (element size:1 in FEMAP) mesh size, F is the compressive force for the actual element size. The result of the mesh density analysis can be seen in Fig. 9.

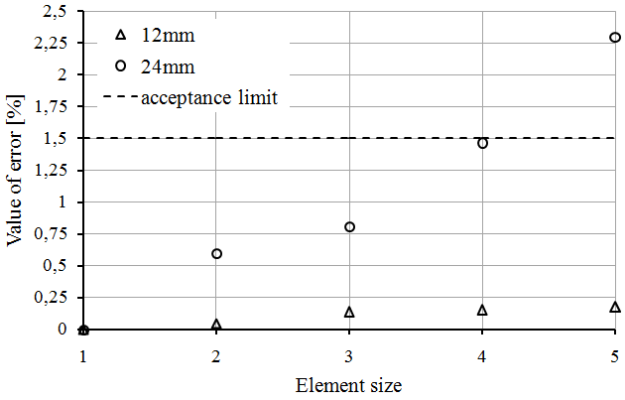

Fig. 9 Mesh density analysis

The strategy was to increase the element size, i.e. to get clearer mesh which gives accurate result while much more cost efficient, considering its time demand, see in Fig. 10.

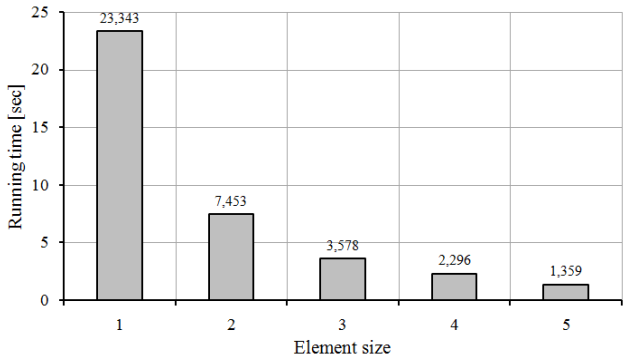

Fig. 10 Numerical analysis on time demand

The air-springs are designed so that the buses can "kneel" at bus stops, and the air-spring goes flat. The rubber bumper rests against the bumper plate at that time. It can be seen in Fig. 11 that the rubber bumper comes into contact with the top plate and the pin even under a small compression. The displacements are known on the lower and upper surfaces. Between the rubber and steel friction is also taken into consideration during the finite element modeling. In Table I the FEM input data are listed.

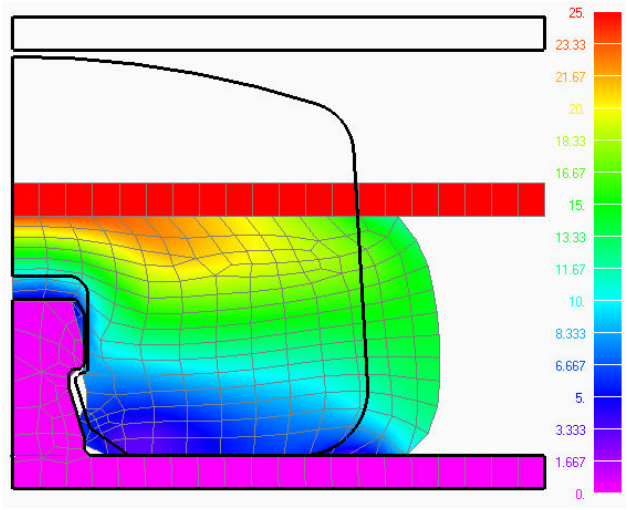

Fig. 11 The initial and the deformed geometry in working conditions

TABLE I
FEM INPUT DATA

Symbol	Quantity	Value
$C_i, i = 1 \dots 9$	Mooney-Rivlin material contants	from Fig. 4
κ	bulk modulus	1000N/mm^2
μ	friction coefficient	0,4
Δu	prescribed displacement increment	1mm
m	number of load steps	25

The load-displacement curve of the rubber bumper is evaluated, see in Fig. 12.

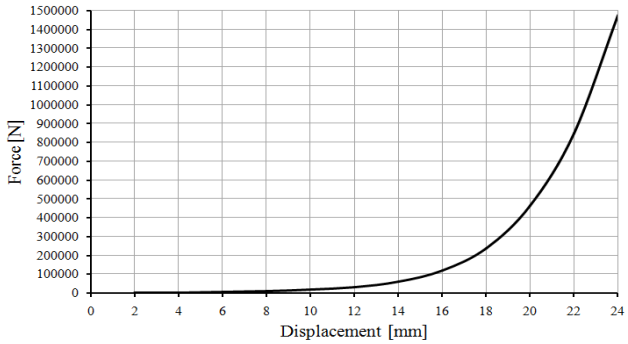

Fig. 12 Load-displacement curve of the rubber bumper

IV. Conclusion

A solution of a contact problem including friction for large displacements and deformations are analyzed where a rubber bumper applied in air-springs is investigated by determining the nonlinear load-displacement curve. As a preparation for the further shape optimization numerical stability and parameter optimization analyses and numerical material constants determination have been performed to reduce the calculation time of the time-consuming finite element computations.

Acknowledgment

The described work was carried out as part of the TÁMOP-4.1.1.C-2012/1/KONV-2012-0012 project in the framework of the New Hungarian Development Plan. The realization of this project is supported by the European Union co-financed by the European Social Fund.

References

[1] T. Mankovits, T. Szabó, I. Kocsis, I. Páczelt, "Optimization of the Shape of Axi-Symmetric Rubber Bumpers," *Strojniski vestnik-Journal of Mechanical Engineering*, vol. 60, no. 1, pp. 61-71, 2014.
[2] T. Mankovits, T. Szabó, "Finite Element Analysis of Rubber Bumper Used in Air-Springs," *Procedia Engineering*, vol. 48, pp. 388-395, 2012.
[3] T. Mankovits, I. Kocsis, T. Portik, T. Szabó, I. Páczelt, "Shape Design of Rubber Part Using FEM," *International Review of Applied Sciences and Engineering*, vol. 4, no. 2, 85-94, 2013.
[4] R.K. Luo, W.X. Wu, "Fatigue Failure Analysis of Antivibration Rubber Spring," *Engineering Failure Analysis*, vol. 13, no. 1, pp. 110-116, 2006.
[5] Q. Li, J. Zhao, B. Zhao, "Fatigue Life Prediction of a Rubber Mount Based on Test of Material Properties and Finite Element Analysis," *Engineering Failure Analysis*, vol. 16, no. 7, pp. 2304-2310, 2009.
[6] S. Oman, M. Fajdiga, M. Nagode, "Estimation of Air-Spring Life Based on Accelerated Experiments," *Materials and Design*, vol. 31, no. 8, pp. 3859-3868, 2010.
[7] S. Oman, M. Nagode, "On the Influence of Cord Angle on Air-Spring Fatigue Life," *Engineering Failure Analysis*, vol. 27, pp. 61-73, 2013.
[8] L.R. Wang, J.C. Wang, I. Hagiwara, "An Integrated Characteristic Simulation Method for Hydraulically Damped Rubber Mount of Vehicle Engines," *Journal of Sound and Vibration*, vol. 286, no. 4-5, pp. 673-696, 2005.
[9] ISO 7743 "Rubber, vulcanized or thermoplastic – Determination of compression stress-strain properties", 2008.